

# DropIT: Dropping Intermediate Tensors for Memory-Efficient DNN Training

Joya Chen <sup>\*1</sup> Kai Xu <sup>\*1</sup> Yifei Cheng <sup>2</sup> Angela Yao <sup>1</sup>

## Abstract

A standard hardware bottleneck when training deep neural networks is GPU memory. The bulk of memory is occupied by caching intermediate tensors for gradient computation in the backward pass. We propose a novel method to reduce this footprint by selecting and caching part of intermediate tensors for gradient computation. Our Intermediate Tensor Drop method (DropIT) adaptively drops components of the intermediate tensors and recovers sparsified tensors from the remaining elements in the backward pass to compute the gradient. Experiments show that we can drop up to 90% of the elements of the intermediate tensors in convolutional and fully-connected layers, saving  $\sim 20\%$  GPU memory during training while achieving higher test accuracy for standard backbones such as ResNet and Vision Transformer. Our code is available at <https://github.com/ChenJoya/dropit>.

## 1. Introduction

The training of state-of-the-art deep neural networks (DNNs) (Krizhevsky et al., 2017; Simonyan & Zisserman, 2015; He et al., 2016; Vaswani et al., 2017; Dosovitskiy et al., 2021) for computer vision often requires large GPU memory. For example, the training forward pass of a small Visual Transformer model ViT-B/16 (Dosovitskiy et al., 2021), with image inputs of  $224 \times 224$  and a standard batch size of 512, requires  $>80$  GB GPU memory. Such large memory requirements make the training of DNNs out of reach for the average deep learning academic or practitioner who does not have access to high-end GPU resources.

When training DNNs, the GPU memory has three primary uses (Chen et al., 2016; Sohoni et al., 2019): **model memory** for storing network parameters, **optimization memory** for buffering the gradients, and **tensor cache** for storing intermediate tensors for gradient computation. In most computer vision tasks, the training input is usually a large batch

<sup>\*</sup>Equal contribution <sup>1</sup>National University of Singapore (NUS) <sup>2</sup>University of Science and Technology of China (USTC). Correspondence to: Joya Chen <joyachen@nus.edu.sg>, Kai Xu <kxu@comp.nus.edu.sg>, Yifei Cheng <chengyif@mail.ustc.edu.cn>, Angela Yao <ayao@comp.nus.edu.sg>.

of high-resolution images or videos, resulting in huge GPU memory consumption in the tensor cache. In the example above, although the training forward pass of the ViT-B/16 model takes up  $>80$ GB of GPU memory, it's testing forward pass only consumes  $\sim 2$  GB GPU memory. Since the testing mode will not save intermediate tensors for gradient computation, the vast gap in GPU memory between training and testing is caused by the tensor cache. Therefore, in previous studies (Feng & Huang, 2021; Gruslys et al., 2016; Chen et al., 2016; Rajbhandari et al., 2020), tensor cache is always considered to be the vast majority of GPU memory consumption.

In this work, we focus on reducing the tensor cache. For differentiable layers like convolution, standard implementations store the input tensors for computing the gradients during back-propagation. One option to reduce storage is to cache tensors from only some layers. Uncached tensors get re-computed on the fly during the backward pass – this is the strategy of gradient checkpointing (Feng & Huang, 2021; Gruslys et al., 2016; Chen et al., 2016). Checkpointing has an obvious computation trade-off, since the forward pass must be performed twice to re-compute any uncached intermediate tensors. Unlike gradient checkpointing reducing tensor cache by re-computation, we propose to *sparsify* the cached intermediate tensors. Our method, namely Dropping Intermediate Tensor (DropIT), can reduce the memory burden in tensor cache and not require re-computation. While gradients computed with these partial tensors are an approximation of gradients computed with the full tensor, we observe that the approximated gradients neither hinder training efficiency nor testing accuracy.

What distinguishes our work is that we drop elements only in the *cached* intermediate tensors, *i.e.* we are not aiming to reduce the model size, and we retain the full intermediate tensors in the forward pass. Instead, we target a smaller cache memory for training and apply the sparsified intermediate tensors to estimate the gradient for model learning. This means DropIT is different from Dropout (Srivastava et al., 2014) because the latter would directly affect the layer's computational results during the forward pass. Moreover, DropIT is also different than sparsification schemes used in distributed training which target the gradient directly to limit communication bandwidth (Lin et al., 2018; Aji & Heafield, 2017).

We design different schemes for selecting the dropping indices, including random sampling and min- $k$  selection based on the tensor magnitude. Experimentally, we show

that learning with updates derived from the approximated gradients computed from min- $k$  dropped intermediate tensors converges similarly and achieves even higher testing accuracies than baselines. At the same time, we reduce the tensor cache by up to 90% on convolutional and fully connected layers, resulting in considerable memory saving during training. We can reduce up to 20% total GPU memory consumption for *e.g.* Visual Transformer (Dosovitskiy et al., 2021).<sup>1</sup>

## 2. Related Work

**Memory-Efficient Training Schemes.** Previous studies (Rajbhandari et al., 2020; Feng & Huang, 2021; Sohoni et al., 2019) have shown that GPU memory during DNN training can be split into three sources: model memory, optimization memory, and tensor cache. The model and optimization memory can be reduced by using lightweight operations (Howard et al., 2017; Xie et al., 2017) to save the memory of model parameters, distributed scheduling (Rajbhandari et al., 2020) to save the memory of optimizer states, and mixed precision (Micikevicius et al., 2018) to save memory for storing gradients.

The last source, tensor cache, occupies an overwhelming proportion of the memory bulk for most vision models for two reasons: first, inputs of vision task always have high resolutions, the input is even larger than thousand pixels for semantic segmentation and de-blurring tasks, causing a magnitude larger tensor size than model weight as convolutional weights are always shared spatially; secondly, the intermediate tensor cache size will be proportional to the batch size. Large batch size is often required to provide more accurate batch statistics for batch normalization, leading to more tensor cache than model storage.

There are two approaches to reduce the tensor cache include Gradient Checkpointing (Chen et al., 2016; Gruslys et al., 2016; Feng & Huang, 2021) and the InPlace-ABN operation (Bulo et al., 2018). Checkpointing stores tensors from only a few layers and recomputes any un-cached tensors again when performing the backward pass; in the extreme case, this is equivalent to duplicating the forward pass, so any memory savings come as an extra computational expense. InPlace-ABN specifically targets batch normalization and removes the need to save intermediate tensors by merging batch normalization and ReLU into a single in-place operation, with some small computational overhead.

Our method differs from the methods above in that we do not

<sup>1</sup>Note that the memory reduction is bounded by the cache proportion in the convolutional/fully connected layers. In a general deep neural network, this ratio is 1/3 as the number of activation and normalization layers is often twice that of convolutional/fully connected layers.

need additional re-computation to reduce the intermediate tensors. We heuristically sparsify the tensors and experimentally show that resulting approximated gradients lead to the same convergence level as the original.

**Gradient Sparsification and Compression.** Approximating gradients has been explored in large-scale distributed training to limit communication bandwidth for gradient exchange. Previous works (Strom, 2015; Dryden et al., 2016; Aji & Heafield, 2017; Lin et al., 2018) propose to drop gradients based on some set thresholds and send only the most significant entries of the stochastic gradient. The dropping saves up to 99% of the gradient exchange with little or no loss in accuracy. (Stich et al., 2018) analyzed SGD with gradient sparsification and proved that it would converge at the same level as vanilla SGD when equipped with error compensation.

While gradient sparsification can largely reduce communication cost, it operates on the weight’s gradient itself and does not address the main memory bottleneck, *i.e.* the cache memory. In contrast, our work drops elements from the intermediate tensors used in computing these gradients; these tensors are cached from the forward pass and occupy the majority of the memory used in learning models such as ResNet (He et al., 2016) and Visual Transformers (Dosovitskiy et al., 2021).

## 3. Methodology

### 3.1. Preliminaries

We denote the forward function and learnable parameters of  $i$ -th layer as  $l$  and  $\theta$ , respectively. In the forward pass,  $l$  operates on the layer’s input  $a$  to compute the output  $z$ :<sup>2</sup>

$$z = l(a, \theta). \quad (1)$$

For example, if layer  $i$  is a convolution layer,  $l$  would indicate a convolution operation with  $\theta$  representing the kernel weights and bias parameter.

Given a loss function  $F(\Theta)$ , where  $\Theta$  represents the parameters of the entire network, the gradient with respect to  $\theta$  at layer  $i$  can be estimated according to the chain rule as

$$\nabla \theta \triangleq \frac{\partial F(\Theta)}{\partial \theta} = \nabla z \frac{\partial z}{\partial \theta} = \nabla z \frac{\partial l(a, \theta)}{\partial \theta}, \quad (2)$$

where  $\nabla z \triangleq \frac{\partial F(\Theta)}{\partial z}$  is the gradient passed back from layer

<sup>2</sup>Note that the input of the  $i$ -th layer is the output from the previous layer  $i-1$ , *i.e.*  $a^i = z^{i-1}$ . However, we assign different symbols to denote the input and output of a given layer explicitly; this redundant notation conveniently allows us, for clarity purposes, to drop explicit reference of the layer index  $i$  as a superscript.

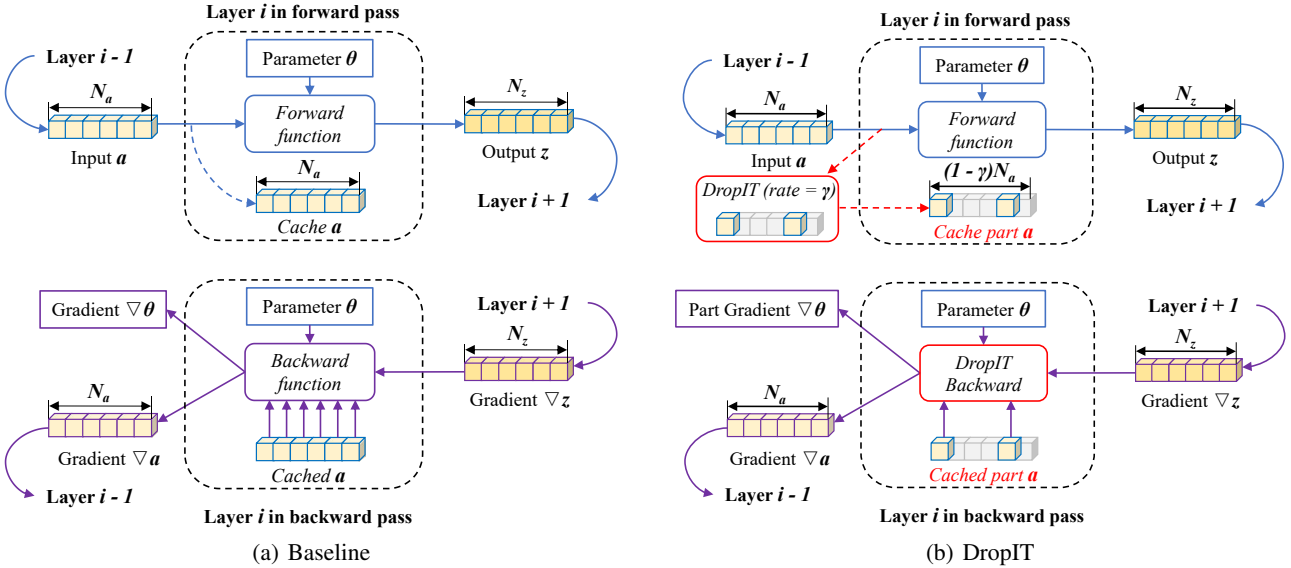


Figure 1. This figure compares common forward/backward pass and forward/backward pass with DropIT. For a regular network, the intermediate tensor is fully cached in the forward pass, which is used for gradient computation during the backward pass. For DropIT, we sparsify intermediate tensors and drop elements during caching. During the backward pass, only saved elements are used for gradient computation. Best viewed in colors.

$i + 1$  layer. Note that the computation of  $\frac{\partial l(a, \theta)}{\partial \theta}$  requires  $a$  if the forward function  $l$  involves tensor multiplication between  $a$  and  $\theta$ . This is the case for many learnable layers, such as convolution and fully-connected layers. As such,  $a$  is necessary for estimating the gradient and is cached after it is computed during the forward pass, as illustrated in Figure 1(a).

The gradient  $\nabla a$  can be estimated similarly via chain rule as

$$\nabla a \triangleq \frac{\partial F(\Theta)}{\partial a} = \nabla z \frac{\partial z}{\partial a} = \nabla z \frac{\partial l(a, \theta)}{\partial a}. \quad (3)$$

Analogous to Eq. 2, the partial  $\frac{\partial l(a, \theta)}{\partial a}$  may depend on  $\theta$  and  $\theta$  is similarly stored in the model memory. Compared to  $a$ , however,  $\theta$  typically occupies much less memory. This is especially true for convolution, as  $\theta$  is shared for different input regions and batch samples. For example, the well-known ResNet-50 requires only  $\sim 98$ MB GPU memory for storing the parameters, but requires  $\sim 18$ GB to cache intermediate tensors when training on ImageNet with a standard batch size 256. The space complexity for model parameters and intermediate tensors are compared in Table 1. The complexity for tensors becomes considerable if batch size  $B$  or feature map size  $H \times W$  is large.

For some layers, *e.g.* batch normalization and ReLU, the partial  $\frac{\partial l(a, \theta)}{\partial a}$  may also depend on  $a$ . In these cases, we do not drop the cache of intermediate tensors as this will affect

| Layer Type      | Parameter $\theta$ | Tensor $a$   |
|-----------------|--------------------|--------------|
| Convolution     | $O(C_a C_z K^2)$   | $O(BC_a HW)$ |
| Fully Connected | $O(C_a C_z)$       | $O(BC_a)$    |

Table 1. **Space complexity** for parameters and intermediate tensors in a single layer.  $B$  denotes batch size,  $C_a, C_z$  are the number of input and output channels,  $K$  is the kernel size, and  $H$  and  $W$  are height and width of the input tensor. Typically,  $H \times W \gg K^2$  and depending on  $B$ , the complexity for intermediate tensors becomes considerable.

subsequent backpropagation, causing aggregated dropping effect on the gradient. For example, the gradient of the first layer will be affected by all the dropping errors and the convolution layers/fully connected layers, which will lead to sub-optimal convergence in the experiment.

Instead, for DropIT, dropping happens only when the gradient flows to the parameters, which prevents the aggregation of the error from the gradient approximation. DropIT could achieve a similar convergence level in this setting if the error caused by dropping is small and bounded.

### 3.2. Dropping Intermediate Tensors

As the layer input  $a$  is required to compute  $\nabla \theta$  (see Equation (2)), it is cached after the forwards pass. We aim to reduce the cache of  $a$  for convolution and fully connected layers by sparsifying this tensor (see comparison in Figure 1(b)).

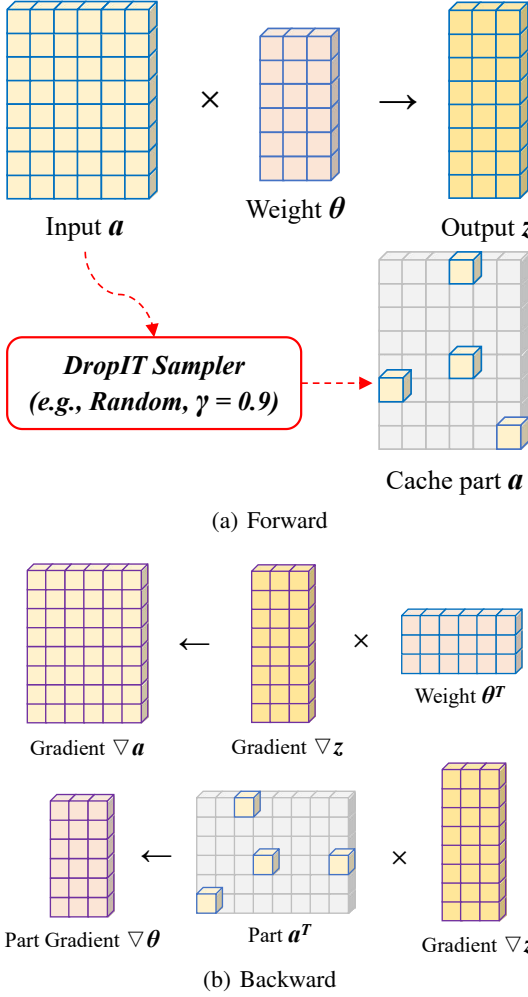


Figure 2. Forward and backward of DropIT on the fully-connected layer (without bias). In the forward pass, we sparsify cache tensor and drop  $\gamma$  percentage storage. In the backward pass, only saved elements will participate the gradient computation.

Consider for a convolutional layer with  $C_z$  kernels of size  $K \times K$ . For the  $j^{\text{th}}$  kernel, where  $j \in [1, C_z]$ , the gradient at location  $(u, v)$  for the  $k^{\text{th}}$  channel is given by

$$\nabla \theta_{j,k}(u, v) = \sum_{(n,x,y) \in \mathcal{X}} \nabla z_j^n(x, y) a_k^n(x', y'), \quad (4)$$

where  $x' = x + u$  and  $y' = y + v$ . The set  $\mathcal{X}$  denotes the set of all sample indices  $n \in [1, B]$  and all location indices  $(x, y) \in [1, W] \times [1, H]$  in the feature map, while index  $k' \in [1, C_a]$  corresponds to the input channel.

Without any loss in generality, we can partition the summation indices of  $\mathcal{X}$  into two disjoint sets  $\mathcal{X}_1$  and  $\mathcal{X}_2$ , where  $\mathcal{X}_1 \cap \mathcal{X}_2 = \emptyset$  and  $\mathcal{X}_1 \cup \mathcal{X}_2 = \mathcal{X}$  to split Equation (4) as

$$\begin{aligned} \nabla \theta_{j,k}(u, v) = & \left[ \sum_{(n,x,y) \in \mathcal{X}_1} \nabla z_j^n(x, y) a_k^n(x', y') \right. \\ & \left. + \underbrace{\sum_{(n,x,y) \in \mathcal{X}_2} \nabla z_j^n(x, y) a_k^n(x', y')}_{\top \theta_{j,k}(u, v)} \right]. \quad (5) \end{aligned}$$

Assume now, that some element  $a_k^n(x', y')$  is very small or near-zero. This element's contribution to the gradient will also be correspondingly small. Intuitively, one can interpret this as having gradients only in spatial locations which are activated during the forward pass. If we assign the spatial indices  $(x, y)$  in sample  $n$  of all such elements to  $\mathcal{X}_1$ , then we can approximate the gradient  $\nabla \theta_{j,k}(u, v)$  with simply the second term of Equation (5). We denote this term, or the approximated gradient, as  $\top \theta_{j,k}(u, v)$ .

For a fully connected layer, the approximated gradient can be defined similarly as

$$\top \theta_{j,k} = \sum_{n \in \mathcal{X}_2} \nabla z_j^n a_k^n. \quad (6)$$

An case of fully-connected layer is shown in Figure 2. With the approximated gradient, we can use any optimizer (e.g., momentum SGD) to update the parameters of this layer. Next, we will cover how to choose which elements to drop.

### 3.3. Dropping Index Selection

The overall dropping rate is defined as  $\gamma = \frac{|\mathcal{X}_2|}{BC_a}$  for a fully connected layer and  $\gamma = \frac{|\mathcal{X}_2|}{BC_a HW}$  for a convolutional layer. The selection of the dropped indices varies in granularity, and can be either individual elements or an entire slice of the tensor corresponding to all the elements for a specific dimension. As we aim for dropping the elements which have minimal contribution to the gradient, it is logical to perform a min- $k$  based selection on the elements' magnitudes and drop them. As a baseline comparison, we also investigate the selection of dropping indices based on uniform random sampling.

We outline the different strategies with various dropping granularities below.

- **Random Channels:** For the intermediate tensors in a mini-batch, we randomly dropped  $\gamma$  channels. For example, if the intermediate tensors have  $C = 256$  channels, with  $\gamma = 0.9$ , we only maintain  $\lfloor (1 - \gamma)C \rfloor = 25$  channels when performing tensor cache.
- **Random Elements:** Similar to Random Channels, for the intermediate tensors in a mini-batch, we randomly

dropped  $\gamma$  elements. We also save the indices of the maintained elements to recover the tensors during the backward pass.

- **Min- $K$  Channels:** Within a mini-batch, we drop channels according to their L2 norm magnitude, and the smallest  $\gamma$  fraction of channels would be dropped. The indices of maintained channels are also recorded.
- **Min- $K$  Elements:** For the intermediate tensors in a mini-batch, the  $\gamma$  fraction of elements with the smallest absolute value are dropped, with the indices of maintained elements recorded. However, this strategy is related to a top- $k$  selection algorithm. If the intermediate tensors are too large, it will cause huge time overhead.
- **Parallel Min- $K$  Elements:** This is a variant of the above Min- $K$  Elements to improve the speed of selection. In Min- $K$  Elements strategy, the smallest  $\gamma$  fraction of elements should be selected, which produces  $O(BCHW)$  time complexity by running a standard top- $k$  algorithm. When the size of the intermediate tensors is too large, the selection step would consume a lot of time. To avoid that, we propose to process every  $D$  ( $D \ll BCHW$ ) elements in parallel, decreasing the time complexity to  $O(D)$ . Although the values discarded in this way are only approximate Min- $K$  elements, we find it can achieve a good trade-off between speed and accuracy by adjusting  $D$ .

### 3.4. A Full Network with DropIT

So far, we have discussed dropping tensors from the cache of a single layer. In theory, DropIT is applicable for all convolutional and fully-connected layers in a network since it does not affect the forward pass operation. In practice, we find that applying DropIT on the first layer results significantly deteriorates the performance. This is because the input to the first layer is often the input data itself. Directly dropping elements or channels of the input data is too extreme, and learning is not effective with the approximated gradient at this first layer. Therefore, we do not apply DropIT to the first convolution layer in the experiments. However, we do modify all remaining convolutional and fully-connected layers to their DropIT version.

## 4. Experiments

### 4.1. Experimental Details

**Datasets & Baseline Models.** We verify our DropIT on the image classification task on CIFAR-100 (Krizhevsky et al., 2009) and ImageNet-1k (Russakovsky et al., 2015). CIFAR-100 comprises 50k training images and 10k test images in 100 classes. ImageNet includes 1000 object classes and

contains 1.2M training images, 50k validation images, and 100k test images. The validation accuracy on the dataset is reported.

For image classification, we experiment with ResNet (He et al., 2016), a 2D CNN, and ViT (Dosovitskiy et al., 2021), a visual transformer. For each model, we compare the classification accuracy, memory cost, speed for training with and without DropIT. For efficient evaluation, we have selected the lightest variant of each model, *i.e.* ResNet-18 (He et al., 2016) and ViT-B/16 (Dosovitskiy et al., 2021).

**Implementation Details.** For ResNet-18 on CIFAR-100, we follow (Zhang et al., 2019) to train the model for 200 epochs with batches of 128 images and decay the learning rate by a factor of 5 at the 60<sup>th</sup>, 120<sup>th</sup> and 160<sup>th</sup> epochs. For ResNet-18 on ImageNet, we use a batch size of 256, learning rate 0.1, and decay the learning rate by a factor of 10 at the 30<sup>th</sup>, 60<sup>th</sup> epochs. The total epochs are 90. We train the model on a single NVIDIA RTX A5000 GPU.

For ViT-B/16 on CIFAR-100 and ImageNet-1k, we follow the configurations from (Dosovitskiy et al., 2021), where the model is finetuned from ImageNet-21k. For CIFAR-100, we use SGD with cosine learning rate decay of an initial learning rate of 0.03, a batch size of 512, to finetune the model for 10<sup>4</sup> steps. For ImageNet-1k, we only change the learning rate of training to 0.01, and finetune the model for 2 × 10<sup>4</sup> steps. We train the model on four NVIDIA RTX A5000 GPUs. For Parallel Min- $K$  dropping, we choose  $D = 2^{14}$  in our experiments, and this value may vary with different GPUs.

In all cases, we maintain the same data augmentation and training strategy for both DropIT and the baseline model. All experiments are implemented with PyTorch by modifying autograd functions (Paszke et al., 2019). We use the commonly used random seed 42.

### 4.2. Ablation Studies

We perform all ablation studies on CIFAR-100 with the ResNet-18 model.

**Dropping Index Granularity.** Table 2 shows that for the same dropping rate  $\gamma$ , channel-wise dropping is always worse than element-wise dropping, regardless of strategy (Random or Min- $K$ ). Furthermore, channel-wise dropping cannot match the baseline performance (71.64 vs. 77.96,  $\gamma = 0.8$ ), whereas element-wise dropping can match and even slightly exceed the baseline (78.78 vs. 77.96,  $\gamma = 0.8$ ). We attribute the accuracy gap to the rough nature of channel-wise dropping, as there are likely to be regions with both small and large gradient contributions within each channel. As element-wise dropping achieves better accuracy than channel-wise dropping, we focus only on the former in the subsequent discussion.

| Index Granularity | Selection Strategy | Dropping Rate $\gamma$ |                |                |                |                |                 | Baseline                |
|-------------------|--------------------|------------------------|----------------|----------------|----------------|----------------|-----------------|-------------------------|
|                   |                    | $\gamma = 0.5$         | $\gamma = 0.6$ | $\gamma = 0.7$ | $\gamma = 0.8$ | $\gamma = 0.9$ | $\gamma = 0.99$ |                         |
| Channels          | Random             | 75.72                  | 75.16          | 74.21          | 73.00          | 70.57          | 11.6            | 77.96<br>646 M<br>62 ms |
|                   |                    | 572 M                  | 542 M          | 510 M          | 474 M          | 448 M          | 426 M           |                         |
|                   |                    | 80 ms                  | 87 ms          | 86 ms          | 77 ms          | 83 ms          | 76 ms           |                         |
|                   | Min-K              | 76.34                  | 75.38          | 74.24          | 71.64          | 67.60          | 18.27           |                         |
|                   |                    | 572 M                  | 542 M          | 510 M          | 474 M          | 448 M          | 426 M           |                         |
|                   |                    | 63 ms                  | 63 ms          | 61 ms          | 59 ms          | 57 ms          | 59 ms           |                         |
| Elements          | Random             | 77.04                  | 76.61          | 75.84          | 74.67          | 73.59          | 64.43           | 77.96<br>646 M<br>62 ms |
|                   |                    | 896 M                  | 802 M          | 709 M          | 602 M          | 512 M          | 434 M           |                         |
|                   |                    | 808 ms                 | 651 ms         | 568 ms         | 336 ms         | 189 ms         | 89 ms           |                         |
|                   | Min-K              | 78.52                  | 78.49          | 78.62          | 78.78          | 78.16          | 65.83           |                         |
|                   |                    | 898 M                  | 840 M          | 710 M          | 602 M          | 512 M          | 434 M           |                         |
|                   |                    | 695 ms                 | 798 ms         | 807 ms         | 813 ms         | 820 ms         | 810 ms          |                         |
|                   | Parallel Min-K     | 78.41                  | 78.44          | 78.59          | <b>78.17</b>   | 77.41          | 66.87           |                         |
|                   |                    | 898 M                  | 812 M          | 710 M          | <b>598 M</b>   | 510 M          | 434 M           |                         |
|                   |                    | 70 ms                  | 69 ms          | 68 ms          | <b>66 ms</b>   | 65 ms          | 63 ms           |                         |

Table 2. Ablation study on dropping granularity, selection strategy, and dropping rate. Reported results are top-1 accuracy, memory cost, and speed of ResNet-18 on CIFAR-100. We highlight DropIT with *Parallel Min-K* in  $\gamma = 0.8$  as in this case, the model achieves higher accuracy than baseline with the best speed and memory performance.

| Dataset   | Method   | Top-1        | Top-5        | Memory (MB)      | Speed (ms) |
|-----------|--|--------------|--------------|------------------|------------|
| CIFAR-100 | ResNet-18 ( $32^2$ ) (He et al., 2016)                           | 77.96        | 94.05        | 648              | 62         |
|           | ResNet-18 ( $32^2$ ) + DropIT (Parallel Min-K, $\gamma = 0.8$ )  | <b>78.17</b> | <b>94.19</b> | 598              | 66         |
|           | ViT-B/16 ( $224^2$ ) (Dosovitskiy et al., 2021)                  | 90.32        | 98.88        | $20290 \times 4$ | 670        |
|           | ViT-B/16 ( $224^2$ ) + DropIT (Parallel Min-K, $\gamma = 0.9$ )  | <b>90.90</b> | <b>99.02</b> | $16052 \times 4$ | 810        |
| ImageNet  | ResNet-18 ( $224^2$ ) (He et al., 2016)                          | 69.76        | 89.08        | 2826             | 108        |
|           | ResNet-18 ( $224^2$ ) + DropIT (Parallel Min-K, $\gamma = 0.8$ ) | <b>69.85</b> | <b>89.39</b> | 2600             | 134        |
|           | ViT-B/16 ( $224^2$ ) (Dosovitskiy et al., 2021)                  | 83.40        | 96.96        | $20290 \times 4$ | 671        |
|           | ViT-B/16 ( $224^2$ ) + DropIT (Parallel Min-K, $\gamma = 0.9$ )  | <b>83.61</b> | <b>97.01</b> | $16056 \times 4$ | 815        |

Table 3. DropIT achieves higher accuracy than baseline with less memory consumption on different backbone networks and datasets. “ $\times 4$ ” means training on 4 GPUs. Settings of memory and speed follow Table 2.

**Dropping Index Strategy.** We have introduced above that dropping elements is better than dropping channels. Now we explore the strategy of dropping elements. As shown in Table 2, for the same dropping rate  $\gamma$ , *Min-K* and *Parallel Min-K* have better accuracy to the baseline with dropping rates  $\gamma = [0.5, 0.8]$ . We speculate the reason for the higher accuracy is that the small values in intermediate tensors lead to small gradients, which may be training noise. *Min-K* and *Parallel Min-K* strategies could reduce the noise in appropriate dropping rate  $\gamma$ . But if  $\gamma$  is too large (e.g.,  $\gamma = 0.99$ ), the DropIT gradient will seriously deviate from the baseline gradient, which would lead to poor accuracy.

If we also consider the speed and memory, *Parallel Min-K* should be the best strategy, especially in  $\gamma = 0.8$ . In this case, the model achieves higher accuracy than baseline with the best speed and memory performance. If  $\gamma > 0.8$ , the memory cost would be larger than baseline due to the extra space allocated by top-k algorithm. So we recommend *Parallel Min-K* with  $\gamma = 0.8$  or  $\gamma = 0.9$  in practice.

### 4.3. Comparison with Baseline Networks

As shown in Table 3, DropIT consistently obtains higher accuracy than baseline for the setting described in the table entries. Our method performs well on ViT-B/16 even in the high dropping rate  $\gamma = 0.9$ , where we achieve  $\sim 20\%$  memory reduction. Note that The activation layer, normalization layer, attention softmax, and query-key-value matrix multiplication in ViT also take up a lot of space. DropIT only works for convolutional and fully-connected layers, so it can only save  $\sim 20\%$  memory instead of  $\sim 90\%$ . Even so, the memory savings and the improved accuracy on ViT have demonstrated the superiority of our approach.

We also observed that DropIT slightly increased time consumption, which is caused by the top-k selection algorithm. We believe that the speed could be further optimized by adapting the optimized top-k algorithm or using sparse matrix multiplication during backward, as we only require  $1 - \gamma$  FLOPs of baseline to accomplish the backward operation.

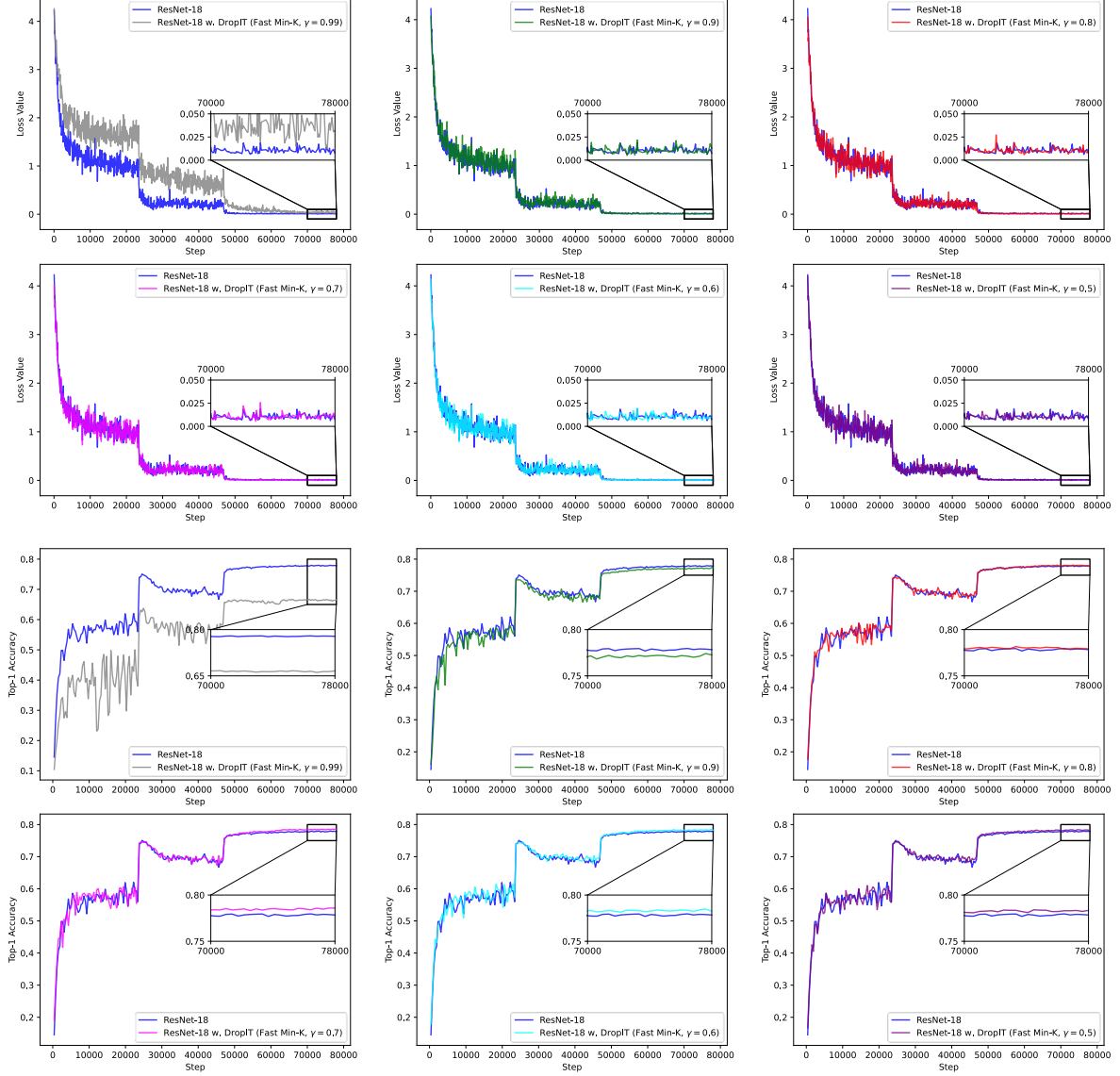
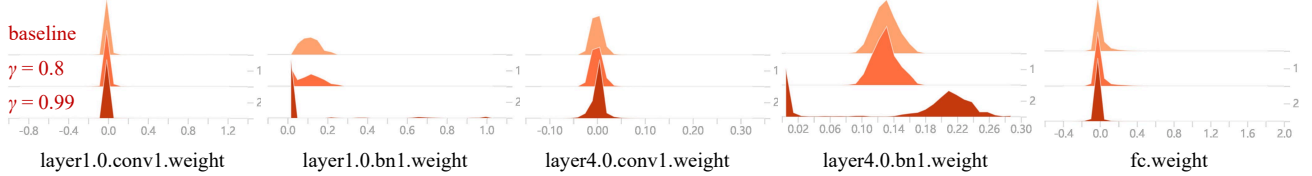


Figure 3. Loss and accuracy plots for ResNet-18 on CIFAR-100 with different dropping ratios.

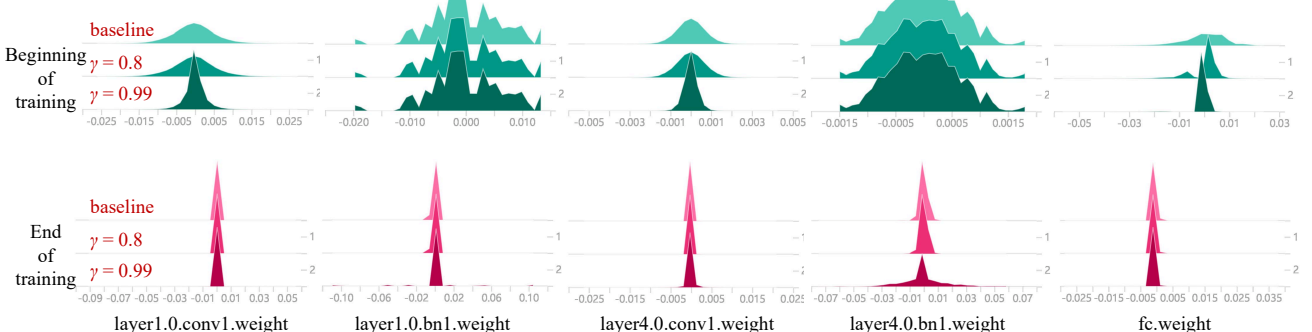
#### 4.4. Gradient and Learning Curve Analysis

**Comparison of Loss Curves.** See Figure 3, we compare the loss curves of baseline ResNet-18 model and ResNet-18 with DropIT of *Parallel Min-K* strategy, in different dropping rate  $\gamma$ . We find that only when  $\gamma = 0.99$ , the loss curve of DropIT has a large gap compared to the baseline. This suggests that dropping 99% elements of intermediate tensors is too difficult for the model to converge to the baseline level. However, in other dropping ratios ( $\gamma = 0.9, 0.8, 0.7, 0.6, 0.5$ ), we find that the loss curves of baseline and DropIT are very similar, even at the end of the training, which demonstrates that DropIT with *Parallel Min-K* strategy can converge to a similar level as the baseline, under an appropriate dropping rate.

**Comparison of Accuracy Curves.** Besides the loss curves, we also compare the accuracy curves of baseline and DropIT of *Parallel Min-K* strategy in Figure 3. Similar to loss curves, we find that only when  $\gamma = 0.99$ , the accuracy curve of DropIT has a large gap compared to the baseline. But in other dropping ratios ( $\gamma = [0.5, 0.9]$ ), their accuracy values are very close. When  $\gamma = [0.5, 0.8]$ , the accuracy of DropIT stably surpasses the accuracy of baseline. As illustrated in Section 4.2, *Parallel Min-K* may reduce the training noise by dropping intermediate elements with small values, thus it can have a stable and better performance in terms of accuracy. In conclusion, both loss and accuracy curves fully prove the value of DropIT, which can save GPU memory without decreasing the model accuracy.



(a) Histogram of parameters.



(b) Histogram of gradients.

Figure 4. Figure (a) compares the parameters histogram for the ResNet-18 model at the beginning of training on the CIFAR-100 dataset. Figure (b) compares the gradients histogram for the ResNet-18 model at the beginning/end of training on the CIFAR-100 dataset. The title of each sub-graph indicates the layer name (shown in PyTorch) in the ResNet-18. Note that  $\gamma = 0.8$  and  $\gamma = 0.9$  is used by the *Parallel Min-K* strategy of DropIT.

**Comparison of Parameters Histogram.** We visualize the histograms of parameters learned from baseline ResNet-18 model and ResNet-18 with DropIT, as shown in Figure 4(a). The parameter distribution for DropIT with  $\gamma = 0.8$  is very close to the baseline distribution at the beginning, middle, and end of the network. Even for DropIT with  $\gamma = 0.99$ , their parameter distributions of convolutional layers remain close. However, we observe that the batch normalization layer is very different from the baseline. This is because a batch normalization layer always follows a convolutional layer, and the former would normalize intermediate tensors of the latter. Thus, the training difference between baseline and DropIT would reflect on the parameters of the batch normalization layer. Once intermediate tensors are normalized, the gradient calculated by them would hardly show the difference from the histogram. This phenomenon also suggests that choosing a suitable  $\gamma$  is necessary.

**Comparison of Gradients Histogram.** Similarly, we visualize the gradient histograms of DropIT and the baseline in Figure 4(b). As we have shown in the comparison of loss curves, the loss plot of DropIT is similar to baseline, which indicates the gradient could be approximated only using 10~20% elements of cache tensor. We verify this observation here by comparing the gradient distributions at the beginning of training (where networks are initialized with the same parameters for all three cases) and the gradient distributions at the end of training (when the network converges).

DropIT with  $\gamma = 0.8$  always shows a good approximation on the gradient of baselines, while DropIT with  $\gamma = 0.99$  shows the difference in the convolutions at the beginning of the training, and in the batch normalization at the end of the training. Due to the normalization effect, the statistical differences in convolutional layers are transferred to batch normalization layers along with the training.

## 5. Conclusion

In this paper, we proposed Dropping Intermediate Tensors (DropIT) method to reduce the GPU memory cost during training DNNs. Specifically, our DropIT drops elements in intermediate tensors for the memory-efficient tensor cache, and it recovers sparsified tensors from the remaining elements in the backward pass to compute the gradient. Our experiments show that DropIT can improve DNNs accuracy and save GPU memory on different backbones and datasets. Compared with gradient checkpointing, our method does not require the re-computation for layers' forward pass. DropIT provides a new perspective to reduce the GPU memory cost during training DNNs.

## References

Aji, A. F. and Heafield, K. Sparse communication for distributed gradient descent. In *EMNLP*, pp. 440–445, 2017.

Bulo, S. R., Porzi, L., and Kortschieder, P. In-place activated batchnorm for memory-optimized training of dnns. In *CVPR*, pp. 5639–5647, 2018.

Chen, T., Xu, B., Zhang, C., and Guestrin, C. Training deep nets with sublinear memory cost. *arXiv*, 1604.06174, 2016.

Dosovitskiy, A., Beyer, L., Kolesnikov, A., Weissenborn, D., Zhai, X., Unterthiner, T., Dehghani, M., Minderer, M., Heigold, G., Gelly, S., Uszkoreit, J., and Houlsby, N. An image is worth 16x16 words: Transformers for image recognition at scale. In *ICLR*, 2021.

Dryden, N., Moon, T., Jacobs, S. A., and Van Essen, B. Communication quantization for data-parallel training of deep neural networks. In *MLHPC workshop*, pp. 1–8, 2016.

Feng, J. and Huang, D. Optimal gradient checkpoint search for arbitrary computation graphs. In *CVPR*, pp. 11433–11442, 2021.

Gruslys, A., Munos, R., Danihelka, I., Lanctot, M., and Graves, A. Memory-efficient backpropagation through time. In *NeurIPS*, pp. 4125–4133, 2016.

He, K., Zhang, X., Ren, S., and Sun, J. Deep residual learning for image recognition. In *CVPR*, pp. 770–778, 2016.

Howard, A. G., Zhu, M., Chen, B., Kalenichenko, D., Wang, W., Weyand, T., Andreetto, M., and Adam, H. Mobilenets: Efficient convolutional neural networks for mobile vision applications. *arXiv:1704.04861*, 2017.

Krizhevsky, A., Hinton, G., et al. Learning multiple layers of features from tiny images. 2009.

Krizhevsky, A., Sutskever, I., and Hinton, G. E. Imagenet classification with deep convolutional neural networks. *Communications of the ACM*, 60(6):84–90, 2017.

Lin, Y., Han, S., Mao, H., Wang, Y., and Dally, B. Deep gradient compression: Reducing the communication bandwidth for distributed training. In *ICLR*, 2018.

Micikevicius, P., Narang, S., Alben, J., Diamos, G. F., Elsen, E., García, D., Ginsburg, B., Houston, M., Kuchaiev, O., Venkatesh, G., and Wu, H. Mixed precision training. In *ICLR*, 2018.

Paszke, A., Gross, S., and Massa, F. e. a. Pytorch: An imperative style, high-performance deep learning library. In *NeurIPS*, pp. 8026–8037, 2019.

Rajbhandari, S., Rasley, J., Ruwase, O., and He, Y. Zero: memory optimizations toward training trillion parameter models. In *SC*, pp. 20, 2020.

Russakovsky, O., Deng, J., Su, H., Krause, J., Satheesh, S., Ma, S., Huang, Z., Karpathy, A., Khosla, A., Bernstein, M. S., Berg, A. C., and Li, F. Imagenet large scale visual recognition challenge. *International Journal of Computer Vision*, 115(3):211–252, 2015.

Simonyan, K. and Zisserman, A. Very deep convolutional networks for large-scale image recognition. In *ICLR*, 2015.

Sohoni, N. S., Aberger, C. R., Leszczynski, M., Zhang, J., and Ré, C. Low-memory neural network training: A technical report. *arXiv:1904.10631*, 2019.

Srivastava, N., Hinton, G. E., Krizhevsky, A., Sutskever, I., and Salakhutdinov, R. Dropout: a simple way to prevent neural networks from overfitting. *J. Mach. Learn. Res.*, 15(1):1929–1958, 2014.

Stich, S. U., Cordonnier, J., and Jaggi, M. Sparsified SGD with memory. In *NeurIPS*, pp. 4452–4463, 2018.

Strom, N. Scalable distributed DNN training using commodity GPU cloud computing. In *INTERSPEECH*, pp. 1488–1492, 2015.

Vaswani, A., Shazeer, N., Parmar, N., Uszkoreit, J., Jones, L., Gomez, A. N., Kaiser, L., and Polosukhin, I. Attention is all you need. In *NeurIPS*, pp. 6000–6010, 2017.

Xie, S., Girshick, R. B., Dollár, P., Tu, Z., and He, K. Aggregated residual transformations for deep neural networks. In *CVPR*, pp. 5987–5995, 2017.

Zhang, M. R., Lucas, J., Ba, J., and Hinton, G. E. Lookahead optimizer: k steps forward, 1 step back. In *NeurIPS*, pp. 9593–9604, 2019.